Journal of Marine Science and Technology

Volume 26 | Issue 6 Article 6

FAST FORWARD-BACKWARD CHANNEL ESTIMATION FOR MIMO STBC-OFDM SYSTEMS

Lena Chang
Department of Communications, Navigation and Control Engineering, National Taiwan Ocean University, Keelung, Taiwan, R.O.C, lenachang@mail.ntou.edu.tw

Recommended Citation
Chang, Lena (2018) "FAST FORWARD-BACKWARD CHANNEL ESTIMATION FOR MIMO STBC-OFDM SYSTEMS," *Journal of Marine Science and Technology*: Vol. 26 : Iss. 6 , Article 6.
DOI: 10.6119/JMST.201812_26(6).0006
Available at: https://jmstt.ntou.edu.tw/journal/vol26/iss6/6

Journal of Marine Science and Technology, Vol. 26, No. 6, pp. 813-825 (2018)
DOI: 10.6119/JMST.201812_26(6).0006

A FAST FORWARD-BACKWARD CHANNEL ESTIMATION FOR MIMO STBC-OFDM SYSTEMS

Lena Chang

Key words: multiple input multiple output (MIMO), space time block code (STBC) orthogonal frequency division multiplexing (OFDM), permutation invariant (PI) property, channel estimation.

ABSTRACT

In the study, we develop a fast forward-backward estimation (FFBE) method for multiple input multiple output (MIMO) space time block code (STBC) orthogonal frequency division multiplexing (OFDM) systems. We examined the matrix structure of the forward-backward (FB) correlation matrix and observed this matrix possessing permutation invariant (PI) property. We also investigated the eigen-property of a matrix with PI property and proved its eigenvectors possessing symmetric property, which can be calculated from two half dimensionality submatrices. Based on these analyses, we propose a fast eigen-decomposition algorithm to reduce the computations required in the eigen-decomposition of FB correlation matrix. Then, the symmetric property of eigenvectors of the forward-backward correlation matrix is applied to develop the FFBE method to reduce the computation complexity in channel estimation. FFBE achieves the same performance as the existing forward-backward averaging (FBA) estimation method (Yu and Lin, 2009) and requires one-fourth computation complexity of FBA. Computer simulations demonstrate the effectiveness and accuracy of the proposed FFBE in channel estimation.

I. INTRODUCTION

Recently, wireless communication techniques have been rapidly developed. For example, Wi-Fi has become an everyday tool for internet access since its reliability and cost effectiveness. As the demand of mobile, broadband and multimedia services increases, it is essential to provide a communication system with higher capacity and faster transmission data rate to satisfy the user's requirements.

Paper submitted 09/06/18; revised 10/22/18; accepted 11/06/18. Author for correspondence: Lena Chang (e-mail: lenachang@mail.ntou.edu.tw).
Department of Communications, Navigation and Control Engineering, National Taiwan Ocean University, Keelung, Taiwan, R.O.C.

Multiple input multiple output (MIMO) wireless systems have been deployed to increase the capacity and reliability of wireless communication systems throughout the world over two decades (Paulraj et al., 2004; Lu et al., 2014; Swindlehurst et al., 2014). Moreover, space-time coding (STC) (Alamouti,1998) techniques and orthogonal frequency division multiplexing (OFDM) (Nee and Prasad, 2000) are considered as the major techniques in wireless communications. STC techniques, such as space-time block coding (STBC) (Tarokh et al., 1999; Wang et al., 2009) as well as space-time trellis coding (STTC) (Tarokh et al., 1998; Hong et al., 2007) exploit the spatial transmitting diversity and improve the reliability of data transmission in wireless communications. The combination of MIMO system with STC creates the space-time signal processing which provides the benefits of diversity and coding gains over single-antenna systems (Naguib et al., 2000; Gesbert et al., 2003). OFDM are considered to be a reliable choice for high rate transmissions and are extensively adopted in various communication standards such as digital video broadcasting (DVB) (Dash et al., 2013), Wi-Fi technologies (IEEE802.11a/g/n/ac) (Doufexi et al., 2002; IEEE Std 802.11, 2016). To avoid inter block interference (IBI) due to the multipath fading channel, the cyclic prefix OFDM (CP-OFDM) (Akansu et al., 1998; Ali et al., 2004) inserts a CP guard interval at the beginning of each OFDM symbol at the transmitter. The available data rate for CP-OFDM would be reduced by the presence of transmission nulls. Then, zero-padding OFDM (ZP-OFDM), a solution to overcome the degradation of CP-OFDM, has been proposed by appending zeros to each OFDM symbol (Muquet et al., 2001). The ZP-OFDM includes the advantages of the CP-OFDM but also guarantees symbol recovery regardless of the channel zero locations. STC-OFDM systems (Lu et al., 2000; Agrawal et al., 1998) combine both coding and modulation techniques to improve the performance of high data-rate wireless communication over wideband channels. STC-OFDM systems efficiently exploiting both the spatial diversity and the frequency-selective-fading diversity acquire lots of attentions. An expectation-maximization (EM) based maximum-likelihood (ML) receiver (Lu et al., 2002) has been designed for STBC-OFDM systems in unknown wireless dispersive fading channels. Some studies (Zhou et al., 2002; Gong et al., 2003) provide channel estimation of STC-OFDM systems. A low-rank Wiener filter-based channel estimator with a significant complexity reduction is proposed in (Gong et al., 2003)

by using the space-time block code (STBC) training pattern. A subspace-based semi-blind channel estimator is developed for the single-user STC-OFDM system (Zhou et al., 2002), which guarantees the multichannel identification ability subject to one or two scalar ambiguities resolved by known pilots. To provide more reliable communications at high speeds, MIMO in combination with OFDM (Sklavos et al., 2002; Zeng et al., 2004; Bolcskei, 2006; Ming and Hanzo, 2007) become the dominant technique for 4G and 5G broadband wireless communications. Combining with the STC, a MIMO STC ZP-OFDM system (Zeng et al., 2006) was developed to improve the system performance in the multiuser environment. A subspace-based blind method has been proposed for estimating the channel impulse responses of an MIMO STC-OFDM system. The subspace-based method utilizing orthogonal property between the noise subspace and channel impulse response, possesses high efficiency in channel estimation by utilizing only a small number of pilots. Then, a semi-blind subspace channel estimation for complex MIMO STC ZP-OFDM system was developed in (Yu and Lin, 2009) to relieve the restriction in (Zeng et al., 2006), which requires the input symbols to be real or complex with symmetry. A forward-backward averaging (FBA) technique was also proposed in (Yu and Lin, 2009) to improve the channel estimation accuracy by using both the forward and backward received data. However, the subspace-based estimation methods (Zeng et al., 2006; Yu and Lin, 2009) suffer the computation burden required in subspace estimation.

In the study, we develop a fast forward-backward estimation (FFBE) method for MIMO STBC ZP-OFDM systems. We examined the structure of correlation matrix formed by the forward and backward received data, and found the symmetric property of the associated eigenvectors. FFBE calculates the noise subspace corresponding to the forward-backward correlation matrix by performing eigen-decomposition of two half-dimensionality matrices which obtained from the combination of received data. In addition, we analyze the computation complexity of the FFBE method in order to understand its speedup performance as compared with FBA and forward-only estimation methods. Simulations show consistent results with the computational analysis.

This paper is organized as follows. The signal model and the subspace-based channel estimation method for MIMO STBC ZP-OFDM systems are illustrated in Section II. In Section III, the eigen-properties of the forward-backward correlation are analyzed. The FFBE method is presented In Section IV. Section V displays the simulation results under various conditions. Finally, the conclusions are given in Section VI.

II. NFIGURATION OF SUBSPACE-BASED CHANNEL ESTIMATIONS

Consider the K-user MIMO OFDM system shown in Fig. 1, which is equipped with two transmitting antennas using Alamouti's STBC scheme at the transmitter and J receiving antennas at the receiver. Assume that all the users are perfectly synchronized in the uplink transmissions. Let $\mathbf{s}_i^{(k)} = \left[s_i^{(k)}(0) \cdots s_i^{(k)}(N-1) \right]^T$

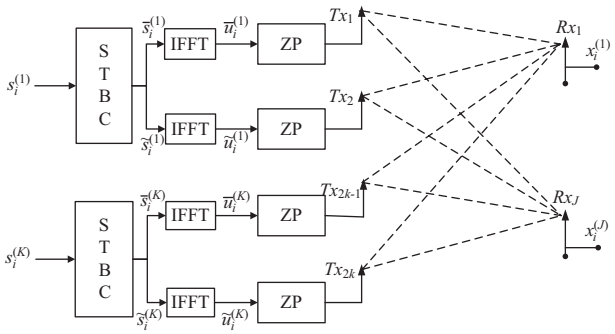

Fig. 1. Multiuser MIMO STBC-based ZP-OFDM system.

be the block symbol of user k transmitted at time i, where N denotes the discrete Fourier transform (DFT) size. $\mathbf{u}_i^{(k)} = \left[u_i^{(k)}(0) \quad \cdots \quad u_i^{(k)}(N-1) \right]^T$ denotes the inverse discrete Fourier transform (IDFT) of $\mathbf{s}_i^{(k)}$. For each user, two consecutive block symbols $\mathbf{s}_{2i}^{(k)}$ and $\mathbf{s}_{2i+1}^{(k)}$ are transmitted across the transmitting antennas according to the following coding scheme:

$$\begin{aligned} \overline{\mathbf{s}}_{2i}^{(k)} &= \mathbf{s}_{2i}^{(k)}, \quad \overline{\mathbf{s}}_{2i+1}^{(k)} = -\left(\mathbf{s}_{2i+1}^{(k)} \right)^*, \\ \tilde{\mathbf{s}}_{2i}^{(k)} &= \mathbf{s}_{2i+1}^{(k)}, \quad \tilde{\mathbf{s}}_{2i+1}^{(k)} = \left(\mathbf{s}_{2i}^{(k)} \right)^* \end{aligned} \tag{1}$$

where $\overline{\mathbf{s}}_i^{(k)}$ and $\tilde{\mathbf{s}}_i^{(k)}$ denote the transmitted blocks through the $(2k-1)^{\text{th}}$ and $(2k)^{\text{th}}$ transmitting antennas, respectively. Let $h^{(j,k)}(l)$, $l = 0, \ldots, L_{j,k}$, be the channel impulse response (CIR) between the kth transmitting antenna and the jth receiving antenna, where $L_{j,k}$ is the channel order and $L_{j,k} \le L$, $k = 1, \ldots, 2K$, $j = 1, \ldots, J$. Before transmitting, the STBC blocks are modulated by the ZP-OFDM to avoid inter block interference (IBI). In ZP-OFDM systems, the ith block symbol is transformed by the IDFT, and then L ($\le N$) zeros are padded at the tail of the transformed block $\overline{\mathbf{u}}_i^{(k)}$ and $\tilde{\mathbf{u}}_i^{(k)}$. Let $\mathbf{x}_i(n) = \left[x_i^{(1)}(n), \ldots, x_i^{(J)}(n) \right]^T$, $n = 0, 1, \ldots, M-1$, be the nth sample vector of the ith OFDM block symbol for all receiving antennas, where $M = L + N$. When the input symbols $\mathbf{s}_i^{(k)}$ are real, the combined receiving signals of MIMO STBC-OFDM systems corresponding to $2i$th and $(2i+1)$th transmitted OFDM blocks are given by

$$\mathbf{r}_i = \begin{bmatrix} \mathbf{x}_{2i} \\ \mathbf{x}_{2i+1} \end{bmatrix} = \begin{bmatrix} \mathbf{H}_1 & \mathbf{H}_2 \\ \mathbf{H}_2 & -\mathbf{H}_1 \end{bmatrix} \begin{bmatrix} \mathbf{u}_{2i} \\ \mathbf{u}_{2i+1} \end{bmatrix} + \begin{bmatrix} \boldsymbol{\eta}_{2i} \\ \boldsymbol{\eta}_{2i+1} \end{bmatrix} \tag{2}$$

In (2), $\mathbf{x}_i = [\mathbf{x}_i^T(0), \mathbf{x}_i^T(1), \ldots, \mathbf{x}_i^T(M-1)]^T \in C^{JM \times 1}$ is the receiving vector at time i; $\mathbf{u}_i = [\mathbf{u}_i^T(0), \mathbf{u}_i^T(1), \ldots, \mathbf{u}_i^T(N-1)]^T \in C^{KN \times 1}$ denotes the ith transformed IDFT block symbol, where

$\mathbf{u}_i(n) = [u_i^{(1)}(n), u_i^{(2)}(n), \ldots, u_i^{(K)}(n)]^T \in C^{K\times 1}$. $\boldsymbol{\eta}_i$ is the additive white Gaussian noise (AWGN), $\boldsymbol{\eta}_i = [\boldsymbol{\eta}_i^T(0), \boldsymbol{\eta}_i^T(1) \ldots, \boldsymbol{\eta}_i^T(M-1)]^T \in C^{JM\times 1}$, where $\boldsymbol{\eta}_i(n) \in C^{J\times 1}$. $\mathbf{H}_j \in C^{JM\times KN}$, j = 1, 2, is a CIR block Toeplitz matrix and given by

$$\mathbf{H}_j = \begin{bmatrix} \mathbf{h}_j(0) & & & \\ \vdots & \mathbf{h}_j(0) & & \\ \mathbf{h}_j(L) & \vdots & \ddots & \\ & \mathbf{h}_j(L) & & \mathbf{h}_j(0) \\ & & \ddots & \vdots \\ & & & \mathbf{h}_j(L) \end{bmatrix} \quad j = 1, 2 \tag{3}$$

where $\mathbf{h}_j(l)$, j = 1, 2, is a $J \times K$ matrix composed of the CIR, given by

$$\mathbf{h}_j(l) = \begin{bmatrix} h^{(1,j)}(l) & h^{(1,2+j)}(l) & \cdots & h^{(1,2K-2+j)}(l) \\ \vdots & \vdots & \ddots & \vdots \\ h^{(J,j)}(l) & h^{(J,2+j)}(l) & \cdots & h^{(J,2K-2+j)}(l) \end{bmatrix} \quad j = 1, 2 \tag{4}$$

In the paper, the noise and transmitted symbols are assumed to satisfy the following statistical properties:

(A1) Noise is white and uncorrelated with zero mean and variance σ_η^2.
(A2) Noise and transmitted symbols are uncorrelated.
(A3) Transmitted symbols are independent and identically distributed (i.i.d.) real random variables, with zero-mean and variance σ_s^2.

According to the above assumptions, we have the correlation matrix of $\mathbf{r}_i$,

$$\mathbf{R}_r = E\left[\mathbf{r}_i \mathbf{r}_i^H\right] = \mathbf{H}\mathbf{R}_v\mathbf{H}^H + \sigma_\eta^2 \mathbf{I}_{2JM} \tag{5}$$

where

$$\mathbf{R}_v = E\left[\mathbf{v}_i \mathbf{v}_i^H\right],\ \mathbf{v}_i = \begin{bmatrix} \mathbf{u}_{2i} \\ \mathbf{u}_{2i+1} \end{bmatrix} \text{ and } \mathbf{H} = \begin{bmatrix} \mathbf{H}_1 & \mathbf{H}_2 \\ \mathbf{H}_2 & -\mathbf{H}_1 \end{bmatrix}.$$

From the subspace decomposition method, it has been shown that

$$\mathbf{e}_k^H \mathbf{H} = 0,\ k = 0, \ldots, q-1 \tag{6}$$

where $q = 2JM - 2KN$, if $\mathbf{H}$ is full column rank. In (6) $\mathbf{e}_k$ is the eigenvector of $\mathbf{R}_r$ corresponding to the smallest eigenvalue σ_η^2 and $\mathbf{e}_k$, $k = 0, \ldots, q-1$, span the left null space of $\mathbf{H}$. As shown in (Zeng et al., 2006), (6) can be rewritten as

$$\mathbf{G}_k \overline{\mathbf{F}} = 0,\ k = 0, \ldots, q-1 \tag{7}$$

Two matrices $\mathbf{G}_k \in C^{N\times 2J(L+1)}$ and $\overline{\mathbf{F}} \in C^{2J(L+1)\times 2K}$ are denoted as

$$\mathbf{G}_k = \begin{bmatrix} \boldsymbol{\alpha}_k^H(L) & \boldsymbol{\alpha}_k^H(L-1) & \cdots & \boldsymbol{\alpha}_k^H(0) \\ \boldsymbol{\alpha}_k^H(L+1) & \boldsymbol{\alpha}_k^H(L) & \cdots & \boldsymbol{\alpha}_k^H(1) \\ \vdots & \vdots & \ddots & \vdots \\ \boldsymbol{\alpha}_k^H(M-1) & \boldsymbol{\alpha}_k^H(M-2) & \cdots & \boldsymbol{\alpha}_k^H(N-1) \end{bmatrix} \tag{8}$$

$$\overline{\mathbf{F}} = \begin{bmatrix} \mathbf{F(0)} \\ \mathbf{F(1)} \\ \vdots \\ \mathbf{F(L)} \end{bmatrix} \tag{9}$$

$$\text{where } \mathbf{F}(l) = \begin{bmatrix} \mathbf{h}_1(l) & \mathbf{h}_2(l) \\ \mathbf{h}_2(l) & -\mathbf{h}_1(l) \end{bmatrix} \in C^{2J\times 2K}$$

In (8), $\mathbf{G}_k$ is composed of transformed eigenvector $\boldsymbol{\alpha}_k = \mathbf{P}\mathbf{e}_k \in C^{2JM\times 1}$, and $\boldsymbol{\alpha}_k$ is partitioned into

$$\boldsymbol{\alpha}_k = \mathbf{P}\mathbf{e}_k = \left[\boldsymbol{\alpha}_k^T(M\text{-}1) \quad \boldsymbol{\alpha}_k^T(M\text{-}2) \quad \cdots \quad \boldsymbol{\alpha}_k^T(0)\right]^T \tag{10}$$

where $\boldsymbol{\alpha}_k(m)$, $m = 0, 1, \ldots, M-1$, is a $2J \times 1$vector. $\mathbf{P}$ defined in (Zeng et al., 2006) satisfies

$$\mathbf{PHQ} = \mathbf{F} = \begin{bmatrix} \mathbf{F}(0) & & & \\ \vdots & \mathbf{F}(0) & & \\ \mathbf{F}(L) & \vdots & \ddots & \\ & \mathbf{F}(L) & & \mathbf{F}(0) \\ & & \ddots & \vdots \\ & & & \mathbf{F}(L) \end{bmatrix} \tag{11}$$

Combining all equations in (7), we have

$$\mathbf{G}\overline{\mathbf{F}} = \mathbf{0} \tag{12}$$

where $\mathbf{G} = \left[G_0^T \ G_1^T \ldots \ G_q^T\right]^T \in C^{qN\times 2J(L+1)}$. Based on the orthogonal property in (12), Zeng (2006) proposed a semi-blind estimation of channel impulse response (CIR) matrix $\mathbf{H}$. Yu and Lin (2009) proposed a forward-backward averaging (FBA)

technique to enhance the performances of blind channel estimation. FBA technique combines the forward and backward signals to calculate the sample correlation matrix, which reduces the random error of the sample correlation matrix and enhances the channel estimation performance. The backward received signal $\mathbf{r}_{b,i}$ is obtained by transforming the received signal $\mathbf{r}_i$ as

$$\mathbf{r}_{b,i} = \begin{bmatrix} -\mathbf{x}_{2i+1} \\ \mathbf{x}_{2i} \end{bmatrix} = \begin{bmatrix} \mathbf{H}_1 & \mathbf{H}_2 \\ \mathbf{H}_2 & -\mathbf{H}_1 \end{bmatrix} \begin{bmatrix} \mathbf{u}_{2i+1} \\ -\mathbf{u}_{2i} \end{bmatrix} + \begin{bmatrix} -\boldsymbol{\eta}_{2i+1} \\ \boldsymbol{\eta}_{2i} \end{bmatrix} \tag{13}$$

From (13), we observe that backward received signal $\mathbf{r}_{b,i}$ has the same CIR matrix as the forward received signal $\mathbf{r}_i$. Moreover, the correlation matrix of backward received signal $\mathbf{r}_{b,i}$ can be expressed as

$$\mathbf{R}_b = E\left[\mathbf{r}_{b,i}\mathbf{r}_{b,i}^H\right] = \mathbf{H}\mathbf{R}_v\mathbf{H}^H + \sigma_\eta^2\mathbf{I}_{2JM} = \mathbf{R}_r \tag{14}$$

(14) indicates that the backward correlation matrix $\mathbf{R}_b$ is same as $\mathbf{R}_r$. The results in (13) and (14) imply that the channel estimation could be performed by employing both forward signal $\mathbf{r}_i$ and backward signal $\mathbf{r}_{b,i}$. The FBA technique combines the forward and backward received signals to get a better estimation of correlation matrix, which is given by

$$\hat{\mathbf{R}}_{fb} = \frac{\hat{\mathbf{R}}_f + \hat{\mathbf{R}}_b}{2} = \frac{1}{2N_s}\sum_{i=0}^{N_s-1}\left(\mathbf{r}_i\mathbf{r}_i^H + \mathbf{r}_{b,i}\mathbf{r}_{b,i}^H\right) \tag{15}$$

where N_s is the number of block signals. It can be shown that $\hat{\mathbf{R}}_{fb}$ is a better estimation of correlation matrix $\mathbf{R}_r$ than $\hat{\mathbf{R}}_f$ in the sense of Euclidean distance, i.e.,

$$\left\|\hat{\mathbf{R}}_{fb} - \mathbf{R}_r\right\| \le \left\|\hat{\mathbf{R}}_f - \mathbf{R}_r\right\|$$

where the Euclidean norm is defined as $\|\mathbf{A}\|^2 = tr(\mathbf{A}^H\mathbf{A})$. Therefore, the eigenvectors corresponding to the forward-backward correlation matrix $\hat{\mathbf{R}}_{fb}$ could achieve better channel estimation than those corresponding to forward only estimation (FOE) (Zeng et al., 2006).

III. EIGEN-STRUCTURE ANALYSIS OF A PERMUTATION INVARIANCE MATRIX

In this section, we examine the structure of the forward-backward sample correlation matrix in (15) and find the symmetric property of the associated eigenvectors. We first observe that the CIR matrix $\mathbf{H}$ shown in (5) has a symmetric structure and satisfies the following permutation invariance (pi) property,

$$\mathbf{M}_{2JM}\begin{bmatrix} \mathbf{H}_1 & \mathbf{H}_2 \\ \mathbf{H}_2 & -\mathbf{H}_1 \end{bmatrix}\mathbf{M}_{2KN} = \begin{bmatrix} \mathbf{H}_1 & \mathbf{H}_2 \\ \mathbf{H}_2 & -\mathbf{H}_1 \end{bmatrix} \tag{16}$$

where $\mathbf{M}_{2t}$ is a $2t \times 2t$ permutation matrix defined as

$$\mathbf{M}_{2t} = \begin{bmatrix} \mathbf{0} & -\mathbf{I}_t \\ \mathbf{I}_t & \mathbf{0} \end{bmatrix} \tag{17}$$

satisfying $\mathbf{M}_{2t}\mathbf{M}_{2t}^T = \mathbf{I}_{2t}$ and $\mathbf{M}_{2t}\mathbf{M}_{2t} = -\mathbf{I}_{2t}$. $\mathbf{I}_t$ denotes a $t \times t$ identity matrix. According to the assumption A3 in Section II, the signal correlation matrix $\mathbf{R}_v$ in (5) can be shown to be a diagonal matrix composed of the signal power. Utilizing the diagonal property of $\mathbf{R}_v$ and (16), we have

$$\begin{aligned} \mathbf{M}_{2JM}\mathbf{R}_r\mathbf{M}_{2JM}^T &= \mathbf{M}_{2JM}(\mathbf{H}\mathbf{R}_v\mathbf{H}^H + \sigma_\eta^2\mathbf{I}_{2JM})\mathbf{M}_{2JM}^T \\ &= \mathbf{M}_{2JM}\mathbf{H}(\mathbf{M}_{2KN}\mathbf{M}_{2KN}^T)\mathbf{R}_v(\mathbf{M}_{2KN}\mathbf{M}_{2KN}^T)\mathbf{H}^H\mathbf{M}_{2JM}^T + \sigma_\eta^2\mathbf{I}_{2JM} \\ &= \mathbf{H}\mathbf{R}_v\mathbf{H}^H + \sigma_\eta^2\mathbf{I}_{2JM} = \mathbf{R}_r \end{aligned} \tag{18}$$

(18) indicates that the correlation matrix $\mathbf{R}_r$ satisfies the the PI property, $\mathbf{M}_{2JM}\mathbf{R}_r\mathbf{M}_{2JM}^T = \mathbf{R}_r$. In reality, the ensemble correlation matrix obtained from the infinite number of received signals is unavailable. Therefore, we apply the sample correlation matrix computed from finite number of signals

$$\hat{\mathbf{R}}_f = \frac{1}{N_s}\sum_{i=0}^{N_s-1}\mathbf{r}_i\mathbf{r}_i^H \tag{19}$$

to channel estimation, where N_s is number of block samples. In addition, we can easily find that the PI property is invalid for sample correlation matrix $\hat{\mathbf{R}}_f$, $\mathbf{M}_{2JM}\hat{\mathbf{R}}_f\mathbf{M}_{2JM}^T \neq \hat{\mathbf{R}}_f$.

The backward received signal $\mathbf{r}_{b,i}$ in (12) can be represented

$$\mathbf{r}_{b,i} = \mathbf{M}_{2JM}\mathbf{r}_i = \begin{bmatrix} -\mathbf{x}_{2i+1} \\ \mathbf{x}_{2i} \end{bmatrix} \tag{20}$$

We observe that $\hat{\mathbf{R}}_{fb}$ possesses the PI property,

$$\mathbf{M}_{2JM}\hat{\mathbf{R}}_{fb}\mathbf{M}_{2JM}^T = \hat{\mathbf{R}}_{fb} \tag{21}$$

The proof is as follows.

$$\begin{aligned} \mathbf{M}_{2JM}\hat{\mathbf{R}}_{fb}\mathbf{M}_{2JM}^T &= \mathbf{M}_{2JM}\left[\frac{\hat{\mathbf{R}}_f + \hat{\mathbf{R}}_b}{2}\right]\mathbf{M}_{2JM}^T \\ &= \mathbf{M}_{2JM}\left[\frac{\hat{\mathbf{R}}_f + \mathbf{M}_{2JM}\hat{\mathbf{R}}_f\mathbf{M}_{2JM}^T}{2}\right]\mathbf{M}_{2JM}^T \\ &= \frac{1}{2}\left[\mathbf{M}\hat{\mathbf{R}}_f\mathbf{M}_{2JM}^T + \mathbf{M}_{2JM}\mathbf{M}_{2JM}\hat{\mathbf{R}}_f\mathbf{M}_{2JM}^T\mathbf{M}_{2JM}^T\right] \\ &= \frac{1}{2}\left[\hat{\mathbf{R}}_b + \hat{\mathbf{R}}_f\right] = \hat{\mathbf{R}}_{fb} \end{aligned}$$

Before analyzing the property of eigenvector of the forward-backward averaging correlation matrix, we first examine the eigen-property of a matrix with PI property. Assume a matrix $\mathbf{S}_T \in C^{2t\times 2t}$ with the following symmetric structure

$$\mathbf{S}_T = \begin{bmatrix} \mathbf{A} & \mathbf{B} \\ -\mathbf{B} & \mathbf{A} \end{bmatrix} \tag{22}$$

where $\mathbf{A}, \mathbf{B} \in C^{t\times t}$. $\mathbf{S}_T$ satisfies the PI property

$$\mathbf{S}_T = \mathbf{M}_{2t}\mathbf{S}_T\mathbf{M}_{2t}^T \tag{23}$$

The eigenvectors of $\mathbf{S}_T$ have the following property.

***Property* 1:** If $\mathbf{e}_i$ is the eigenvector of $\mathbf{S}_T$ with corresponding eigenvalue λ_i, then $\mathbf{Me}_i$ is also the eigenvector of $\mathbf{S}_T$ with eigenvalue λ_i. For a double repeated eigenvalue λ_i, the two corresponding eigenvectors are $\mathbf{e}_i$ and $\mathbf{Me}_i$. If eigenvalue λ_i is not repeated, then the associated eigenvector satisfies the relations

$$\mathbf{e}_i = j\mathbf{M}_{2t}\mathbf{e}_i \text{ or } \mathbf{e}_i = -j\mathbf{M}_{2t}\mathbf{e}_i. \tag{24}$$

Proof:

Since $\mathbf{e}_i$ is the eigenvector of $\mathbf{S}_T$, we have

$$\mathbf{S}_T\mathbf{e}_i = \lambda_i\mathbf{e}_i \tag{25}$$

Pre-multiplying (25) by the permutation matrix $\mathbf{M}_{2t}$ and utilizing the PI property in (23), we get

$$\mathbf{M}_{2t}\mathbf{S}_T\mathbf{M}_{2t}^T\mathbf{M}_{2t}\mathbf{e}_i = \mathbf{S}_T(\mathbf{M}_{2t}\mathbf{e}_i) = \lambda_i(\mathbf{M}_{2t}\mathbf{e}_i) \tag{26}$$

(26) shows that $\mathbf{M}_{2t}\mathbf{e}_i$ is also the eigenvector of $\mathbf{S}_T$ with eigenvalue λ_i. We assume that the eigenvector can be represented as $\mathbf{e}_i = k\mathbf{M}_{2t}\mathbf{e}_i$ if eigenvalue λ_i is not repeated, where k is a scalar. For convenience, we rewrite $\mathbf{e}_i$ as

$$\mathbf{e}_i = \begin{bmatrix} \mathbf{e}_{i1} \\ \mathbf{e}_{i2} \end{bmatrix} = k\begin{bmatrix} 0 & -\mathbf{I}_t \\ \mathbf{I}_t & 0 \end{bmatrix}\begin{bmatrix} \mathbf{e}_{i1} \\ \mathbf{e}_{i2} \end{bmatrix} = k\begin{bmatrix} -\mathbf{e}_{i2} \\ \mathbf{e}_{i1} \end{bmatrix} \tag{27}$$

where $\mathbf{e}_{i1}$ and $\mathbf{e}_{i2} \in C^{t\times 1}$. From (27), we may derive $\mathbf{e}_{i1} = -k^2\mathbf{e}_{i1}$, and get $k = \pm j$, $j = \sqrt{-1}$. The result indicates that if the eigenvalue λ_i is not repeated, the associated eigenvector satisfies the relation in (24).

Then we derive the eigenvectors of the matrix $\mathbf{S}_T$ with PI property by utilizing the following lemma which is proved in Appendix A.

***Lemma* 1**: A matrix $\mathbf{S}_T \in C^{2t\times 2t}$ has the symmetric structure as (22) and satisfies the PI property in (23). The eigenvalues λ_i and the corresponding eigenvector $\mathbf{e}_i$ of $\mathbf{S}_T$ can be obtained from the eigencomponents of two submatrices $(\mathbf{A}+j\mathbf{B})$ and $(\mathbf{A}-j\mathbf{B})$. The eigenvalues are given as follows.

$$\{\lambda_i, i = 1, \ldots, 2t\} = \{\lambda_{\omega,i}, \omega = a, b, i = 1, \ldots, t\}$$

The associated eigenvectors are obtained by

$$\mathbf{e}_i = \begin{bmatrix} \mathbf{e}_{ai} \\ j\mathbf{e}_{ai} \end{bmatrix} \text{ for eigenvalue } \lambda_i = \lambda_{a,i} \tag{28a}$$

or

$$\mathbf{e}_i = \begin{bmatrix} \mathbf{e}_{bi} \\ -j\mathbf{e}_{bi} \end{bmatrix} \text{ for eigenvalue } \lambda_i = \lambda_{b,i} \tag{28b}$$

where $\lambda_{a,i}$ and $\mathbf{e}_{ai}$ are the eigenvalue and associated eigenvector of matrix $(\mathbf{A}+j\mathbf{B})$; $\lambda_{b,i}$ and $\mathbf{e}_{bi}$ are the eigenvalue and associated eigenvector of matrix $(\mathbf{A}-j\mathbf{B})$ respectively.

Lemma 1 shows the eigen-components of matrix $\mathbf{S}_T \in C^{2t\times 2t}$ can be calculated from two submatrices $(\mathbf{A}+j\mathbf{B})$ and $(\mathbf{A}-j\mathbf{B}) \in C^{t\times t}$. By the way, we may reduce the computations required in performing the eigen-decomposition of forward-backward correlation matrix $\hat{\mathbf{R}}_{fb}$.

IV. FAST FORWARD-BACKWARD ESTIMATION METHOD

In the section, the eigen-properties derived in Section III are applied to develop a fast forward-backward estimation (FFBE) method for the channel estimation of MIMO STBC-OFDM systems.

We first explore the symmetric structure of forward-backward correlation matrix with PI property as shown in the *Lemma* 1 and develop a fast eigen-decomposition for the associated eigenvector calculation of $\hat{\mathbf{R}}_{fb}$.

$\hat{\mathbf{R}}_{fb}$ in (14) can be rewritten as

$$\hat{\mathbf{R}}_{fb} = \frac{1}{2N_s}\sum_{i=0}^{N_s-1}\left\{\begin{bmatrix} \mathbf{x}_{2i} \\ \mathbf{x}_{2i+1} \end{bmatrix}\begin{bmatrix} \mathbf{x}_{2i}^H & \mathbf{x}_{2i+1}^H \end{bmatrix} + \begin{bmatrix} -\mathbf{x}_{2i+1} \\ \mathbf{x}_{2i} \end{bmatrix}\begin{bmatrix} -\mathbf{x}_{2i+1}^H & \mathbf{x}_{2i}^H \end{bmatrix}\right\} \tag{29}$$

$\hat{\mathbf{R}}_{fb}$ possesses the symmetric structure as $\mathbf{S}_T$ in (22). The corresponding sub-matrices $\mathbf{A}$ and $\mathbf{B}$ of $\hat{\mathbf{R}}_{fb}$ are given by

$$\mathbf{A} = \frac{1}{2N_s}\sum_{i=0}^{N_s-1}\mathbf{x}_{2i}\mathbf{x}_{2i}^H + \mathbf{x}_{2i+1}\mathbf{x}_{2i+1}^H \tag{30}$$

$$\mathbf{B} = \frac{1}{2N_s}\sum_{i=0}^{N_s-1} \mathbf{x}_{2i}\mathbf{x}_{2i+1}^H - \mathbf{x}_{2i+1}\mathbf{x}_{2i}^H \tag{31}$$

According to *Lemma* 1, we can compute the eigecomponents of $\hat{\mathbf{R}}_{fb}$ from those of $(\mathbf{A}+j\mathbf{B})$ and $(\mathbf{A}-j\mathbf{B})$, which are given by

$$\begin{aligned}\mathbf{A}+j\mathbf{B} &= \frac{1}{2N_s}\sum_{i=0}^{N_s-1}\left(\mathbf{x}_{2i}\mathbf{x}_{2i}^H + \mathbf{x}_{2i+1}\mathbf{x}_{2i+1}^H + j\mathbf{x}_{2i}\mathbf{x}_{2i+1}^H - j\mathbf{x}_{2i+1}\mathbf{x}_{2i}^H\right)\\ &= \frac{1}{2N_s}\sum_{i=0}^{N_s-1}\mathbf{y}_{ai}\mathbf{y}_{ai}^H\end{aligned} \tag{32}$$

$$\begin{aligned}\mathbf{A}-j\mathbf{B} &= \frac{1}{2N_s}\sum_{i=0}^{N_s-1}\left(\mathbf{x}_{2i}\mathbf{x}_{2i}^H + \mathbf{x}_{2i+1}\mathbf{x}_{2i+1}^H - j\mathbf{x}_{2i}\mathbf{x}_{2i+1}^H + j\mathbf{x}_{2i+1}\mathbf{x}_{2i}^H\right)\\ &= \frac{1}{2N_s}\sum_{i=0}^{N_s-1}\mathbf{y}_{bi}\mathbf{y}_{bi}^H\end{aligned} \tag{33}$$

where

$$\mathbf{y}_{ai} = \mathbf{x}_{2i} - j\mathbf{x}_{2i+1} \text{ and } \mathbf{y}_{bi} = \mathbf{x}_{2i} + j\mathbf{x}_{2i+1} \tag{34}$$

By performing eigen-decomposition of correlation matrices $(\mathbf{A}+j\mathbf{B})$ and $(\mathbf{A}\text{-}j\mathbf{B})$ defined in (32) and (33), respectively, we can get the eigenvectors of $\hat{\mathbf{R}}_{fb}$ according to *Lemma* 1.

We then employ the symmetric property of eigenvectors of forward-backward correlation matrix and propose the FFBE method to reduce the computation complexity of channel estimation. The proposed FFBE is developed by considering the eigenvectors of two submatrices $(\mathbf{A}+j\mathbf{B})$ and $(\mathbf{A}-j\mathbf{B})$, respectively.

For eigenvectors $\mathbf{e}_k$ calculated from the eigenvector $\mathbf{e}_{ak}$ of submatrices $(\mathbf{A}+j\mathbf{B})$, we have $\mathbf{e}_k = \begin{bmatrix}\mathbf{e}_{ak}\\ j\mathbf{e}_{ak}\end{bmatrix}$, $k = 1, \ldots, q/2$. Substitute this eigenvectors $\mathbf{e}_k$ into (9), we have

$$\begin{aligned}\boldsymbol{\alpha}_k^H &= \begin{bmatrix}\mathbf{e}_{ak}^H & -j\mathbf{e}_{ak}^H\end{bmatrix}\mathbf{P}^H\\ &= \begin{bmatrix}\boldsymbol{\alpha}_k^H(M\text{-}1) & \boldsymbol{\alpha}_k^H(M\text{-}2) & \cdots & \boldsymbol{\alpha}_k^H(0)\end{bmatrix}\end{aligned} \tag{35}$$

where $\boldsymbol{\alpha}_k^H(m) = \begin{bmatrix}\boldsymbol{\alpha}_{a,k}^H(m) & -j\boldsymbol{\alpha}_{a,k}^H(m)\end{bmatrix} \in C^{J\times 1}$ and matrix $\mathbf{G}_k$ in (7) becomes

$$\mathbf{G}_k = \begin{bmatrix} \boldsymbol{\alpha}_{a,k}^H(L) & -j\boldsymbol{\alpha}_{a,k}^H(L) & \boldsymbol{\alpha}_{a,k}^H(L-1) & -j\boldsymbol{\alpha}_{a,k}^H(L-1) & \cdots & \boldsymbol{\alpha}_{a,k}^H(0) & -j\boldsymbol{\alpha}_{a,k}^H(0)\\ \boldsymbol{\alpha}_{a,k}^H(L+1) & -j\boldsymbol{\alpha}_{a,k}^H(L+1) & \boldsymbol{\alpha}_{a,k}^H(L) & -j\boldsymbol{\alpha}_{a,k}^H(L) & \cdots & \boldsymbol{\alpha}_{a,k}^H(1) & -j\boldsymbol{\alpha}_{a,k}^H(1)\\ \vdots & & \vdots & & \ddots & \vdots & \\ \boldsymbol{\alpha}_{a,k}^H(M-1) & -j\boldsymbol{\alpha}_{a,k}^H(M-1) & \boldsymbol{\alpha}_{a,k}^H(M-2) & -j\boldsymbol{\alpha}_{a,k}^H(M-2) & \cdots & \boldsymbol{\alpha}_{a,k}^H(N-1) & -j\boldsymbol{\alpha}_{a,k}^H(N-1)\end{bmatrix}$$

$k = 0, \ldots, q/2-1.$ (36)

Substituting (35) into (6), we observe that the left half and right half part of *i*th row of $\mathbf{G}_k\bar{\mathbf{F}}$ become

$$\begin{aligned}\sum_{l=0}^{L}\boldsymbol{\alpha}_{a,k}^H(m-l)\mathbf{h}_1(l) - j\boldsymbol{\alpha}_{a,k}^H(m-l)\mathbf{h}_2(l) &= \mathbf{0}\\ \sum_{l=0}^{L}\boldsymbol{\alpha}_{a,k}^H(m-l)\mathbf{h}_2(l) + j\boldsymbol{\alpha}_{a,k}^H(m-l)\mathbf{h}_1(l) &= \mathbf{0}\end{aligned} \tag{37}$$

$$m = L, \ldots, M-1 \tag{38}$$

It is obvious that the solutions of (38) are equivalent to those of (37). Therefore, we solve the CIR by using left half columns of $\mathbf{G}_k\bar{\mathbf{F}}$, which are rearranged as

$$\begin{bmatrix}\mathbf{E}_{ak} & -j\mathbf{E}_{ak}\end{bmatrix}\begin{bmatrix}\mathbf{F}_1\\ \mathbf{F}_2\end{bmatrix} = \mathbf{0} \tag{39}$$

where

$$\mathbf{E}_{ak} = \begin{bmatrix}\boldsymbol{\alpha}_{a,k}^H(L) & \boldsymbol{\alpha}_{a,k}^H(L-1) & \cdots & \boldsymbol{\alpha}_{a,k}^H(0)\\ \boldsymbol{\alpha}_{a,k}^H(L+1) & \boldsymbol{\alpha}_{a,k}^H(L) & \cdots & \boldsymbol{\alpha}_{a,k}^H(1)\\ \vdots & \vdots & & \vdots\\ \boldsymbol{\alpha}_{a,k}^H(M-1) & \boldsymbol{\alpha}_{a,k}^H(M-2) & \cdots & \boldsymbol{\alpha}_{a,k}^H(N-1)\end{bmatrix} \in C^{N\times J(L+1)},$$

and

$$\mathbf{F}_i = \begin{bmatrix}\mathbf{h}_i(o)\\ \mathbf{h}_i(1)\\ \vdots\\ \mathbf{h}_i(L)\end{bmatrix} \in C^{J(L+1)\times K},\ i = 1, 2.$$

Eq. (39) could be reduced to

$$\begin{aligned}&\mathbf{E}_{ak}(\mathbf{F}_1 - j\mathbf{F}_2) = \mathbf{0}\\ &k = 0, \ldots, q/2-1.\end{aligned} \tag{40}$$

Combining all equations in (40), we have

$$\mathbf{E}_a\mathbf{F}_a = \mathbf{0} \tag{41}$$

where

$$\mathbf{E}_a = \begin{bmatrix}\mathbf{E}_{a0}\\ \mathbf{E}_{a1}\\ \vdots\\ \mathbf{E}_{a(q/2-1)}\end{bmatrix} \in C^{\frac{q}{2}N\times J(L+1)}$$

and

$$\mathbf{F}_a = \mathbf{F}_1 - j\mathbf{F}_2 .$$

For eigenvectors $\mathbf{e}_k$ calculated from the eigenvector of submatrix $(\mathbf{A} - j\mathbf{B})$, $\mathbf{e}_{bk}$, we have $\mathbf{e}_k = \begin{bmatrix} \mathbf{e}_{bk} \\ -j\mathbf{e}_{bk} \end{bmatrix}$, $k = 0, \ldots, q/2 - 1$. Similarily as Eq. (35) to (41), $\mathbf{G}_k \bar{\mathbf{F}} = \mathbf{0}$ can be reduced to

$$\begin{bmatrix} \mathbf{E}_{bk} & +j\mathbf{E}_{bk} \end{bmatrix} \begin{bmatrix} \mathbf{F}_1 \\ \mathbf{F}_2 \end{bmatrix} = \mathbf{E}_{bk}(\mathbf{F}_1 + j\mathbf{F}_2) == \mathbf{0} \quad k = 1, \ldots, \mathrm{q}/2. \tag{42}$$

where

$$\mathbf{E}_{bk} = \begin{bmatrix} \boldsymbol{\alpha}_{b,k}^H(L) & \boldsymbol{\alpha}_{b,k}^H(L-1) & \cdots & \boldsymbol{\alpha}_{b,k}^H(0) \\ \boldsymbol{\alpha}_{b,k}^H(L+1) & \boldsymbol{\alpha}_{b,k}^H(L) & \cdots & \boldsymbol{\alpha}_{b,k}^H(1) \\ \vdots & \vdots & & \vdots \\ \boldsymbol{\alpha}_{b,k}^H(M-1) & \boldsymbol{\alpha}_{b,k}^H(M-2) & \cdots & \boldsymbol{\alpha}_{b,k}^H(N-1) \end{bmatrix} \in C^{N \times J(L+1)},$$

$$\boldsymbol{\alpha}_k = \mathbf{P}\begin{bmatrix} \mathbf{e}_{bk} \\ -j\mathbf{e}_{bk} \end{bmatrix} \text{ and } \boldsymbol{\alpha}_k^H(m) = \begin{bmatrix} \boldsymbol{\alpha}_{b,k}^H(m) & j\boldsymbol{\alpha}_{b,k}^H(m) \end{bmatrix}.$$

Combine the equations in (42) for k = 1, …, q/2 and get

$$\mathbf{E}_b \mathbf{F}_b = \mathbf{0} \tag{43}$$

where

$$\mathbf{E}_b = \begin{bmatrix} \mathbf{E}_{b0} \\ \mathbf{E}_{b1} \\ \vdots \\ \mathbf{E}_{b(q/2-1)} \end{bmatrix} \in C^{\frac{q}{2}N \times J(L+1)}$$

and

$$\mathbf{F}_b = \mathbf{F}_1 + j\mathbf{F}_2 .$$

The least square solutions of $\mathbf{F}_a$ and $\mathbf{F}_b$ in (41) and (43) can be estimated by the right null subspace of $\mathbf{E}_a$ and $\mathbf{E}_b$, respectively. According to the identification analysis shown in (Zeng et al., 2006), the estimated $\mathbf{F}_a$ and $\mathbf{F}_b$ are expressed as

$$\hat{\mathbf{F}}_a = \mathbf{V}_a \mathbf{C}_a \text{ and } \hat{\mathbf{F}}_b = \mathbf{V}_b \mathbf{C}_b \tag{44}$$

where $\mathbf{V}_i \in C^{J(L+1) \times K}$, $i = a, b,$ is formed by K right singular vectors corresponding to the K smallest singular values of $\mathbf{E}_i$, $i = a, b$. In (44), $\mathbf{C}_i \in C^{K \times K}$, $i = a, b$, is an ambiguity matrix which can be resolved by using a few pilot symbols (Zeng et al., 2006). Divide $\mathbf{V}_i$ into $(L+1)$ blocks, $\mathbf{V}_i = [\mathbf{V}_i^T(0), \mathbf{V}_i^T(1), \ldots, \mathbf{V}_i^T(L)]^T$, and (44) becomes

$$\begin{aligned} \hat{\mathbf{F}}_a(l) &= \mathbf{h}_1(l) - j\mathbf{h}_2(l) = \mathbf{V}_a(l)\mathbf{C}_a, \\ \hat{\mathbf{F}}_b(l) &= \mathbf{h}_1(l) + j\mathbf{h}_2(l) = \mathbf{V}_b(l)\mathbf{C}_b, \end{aligned} \quad l = 0, 1, \ldots L. \tag{45}$$

Combining the equations in (45), we have

$$\begin{aligned} \mathbf{g}_1(0) - j\mathbf{g}_2(0) &= \mathbf{W}_a \mathbf{C}_a, \\ \mathbf{g}_1(0) + j\mathbf{g}_2(0) &= \mathbf{W}_b \mathbf{C}_b. \end{aligned} \tag{46}$$

where $\mathbf{W}_i = \sum_{i=0}^{L} \mathrm{V}_i(l)$, $i = a, b,$ and $\mathbf{g}_i(0) = \sum_{\mathrm{i}=0}^{\mathrm{L}} \mathbf{h}_i(l)$, $i = 1, 2,$ represents the DFT of CIR and can be estimated by pilot symbols. From (46), we obtained the ambiguity matrix,

$$\begin{aligned} \mathbf{C}_a &= (\mathbf{W}_a^H \mathbf{W}_a)^{-1} \mathbf{W}_a^H [\mathbf{g}_1(0) - j\mathbf{g}_2(0)] \\ \mathbf{C}_b &= (\mathbf{W}_b^H \mathbf{W}_b)^{-1} \mathbf{W}_b^H [\mathbf{g}_1(0) + j\mathbf{g}_2(0)\ ] \end{aligned} \tag{47}$$

Substitute (47) into (44), we get the estimated $\hat{\mathbf{F}}_a$ and $\hat{\mathbf{F}}_b$. Then, the CIR are obtained from (45),

$$\begin{aligned} \mathbf{h}_1(l) &= [\hat{\mathbf{F}}_a(l) + \hat{\mathbf{F}}_b(l)]/2 \\ \mathbf{h}_2(l) &= [\hat{\mathbf{F}}_a(l) - \hat{\mathbf{F}}_b(l)]/j2 \end{aligned} \quad l = 0, 1, \ldots L. \tag{48}$$

The proposed FFBE method is summarized as follows:

1. Form two signals

$$\mathbf{y}_{ai} = \mathbf{x}_{2i} - j\mathbf{x}_{2i+1} \text{ and } \mathbf{y}_{bi} = \mathbf{x}_{2i} + j\mathbf{x}_{2i+1}$$

   from two consecutive received block signals $\mathbf{x}_i$.
2. Compute the correlation matrices of $\mathbf{y}_{ai}$ and $\mathbf{y}_{bi}$, and get $(\mathbf{A} + j\mathbf{B})$ and $(\mathbf{A} - j\mathbf{B})$ according to (32) and (33).
3. Perform eigen-decomposition of correlation matrices $(\mathbf{A} + j\mathbf{B})$ and $(\mathbf{A} - j\mathbf{B})$, and get the eigencomponents which satisfy $(\mathbf{A} + j\mathbf{B})\mathbf{e}_{ak} = \lambda_{a,k}\mathbf{e}_{ak}$ and $(\mathbf{A} - j\mathbf{B})\mathbf{e}_{bk} = \lambda_{b,k}\mathbf{e}_{bk}$.
4. Utilize the eigenvectors $\mathbf{e}_{ak}$ and $\mathbf{e}_{bk}$ in Step 3 to form matrix $\mathbf{E}_a$ and $\mathbf{E}_b$ according to (40) and (42). Perform singular value decomposition of $\mathbf{E}_a$ and $\mathbf{E}_b$, and choose K right side singular vector corresponding to the K smallest singular values to form $\mathbf{V}_a$ and $\mathbf{V}_b$.
5. Apply $\mathbf{V}_a$ and $\mathbf{V}_b$ obtained in Step 4 to estimate $\mathbf{F}_a$ and $\mathbf{F}_b$. Then, the CIR $\mathbf{h}_i(l)$, i = 1, 2, l = 0, …, L, could be obtained by using (48).

From the above derivations, we have proved that the eigenvectors of $\hat{\mathbf{R}}_{fb}$ computed by FFBE are equivalent to those obtained by eigen-decomposition of $\hat{\mathbf{R}}_{fb}$. And the CIR $\mathbf{h}_i(l)$ estimated by FFBE are the same as those by FBA. However, the dimension of matrices $(\mathbf{A}+j\mathbf{B})$ and $(\mathbf{A}-j\mathbf{B})$ applied in FFBE is half of that of $\hat{\mathbf{R}}_{fb}$ required in FBA. In the following, we compare the computation complexity of the proposed FFBE with FBA. For FFBE, it requires $2N_s \times (JM)^2$ multiplications in forming the matrices $(\mathbf{A}+j\mathbf{B})$ and $(\mathbf{A}-j\mathbf{B})$ according to (32) and (33), and $2\times O((JM)^3)$ multiplications in performing eigen-decomposition of $(\mathbf{A}+j\mathbf{B})$ and $(\mathbf{A}-j\mathbf{B})$. Whereas, FBA needs $2N_s \times (2JM)^2 = 8N_s \times (JM)^2$ and $O((2JM)^3)$ multiplications in forming the correlation matrix $\hat{\mathbf{R}}_{fb}$ shown in (15) and performing eigen-decomposition of $\hat{\mathbf{R}}_{fb}$. Thus, we know that the multiplications required in performing eigen-decomposition of FFBE given in step 1-3 are one fourth of that required in FBA. Moreover, since the dimension of $\mathbf{E}_a$ and $\mathbf{E}_b$, given by $(q/2)N \times J(L+1)$, is also one half of matrix $\mathbf{G}$, with dimension equal to $qN \times 2J(L+1)$, the computations required in performing SVD of $\mathbf{E}_a$ and $\mathbf{E}_b$ is almost one fourth of that required in doing SVD of $\mathbf{G}$. As a whole, the computation complexity of FFBE is almost one fourth of FBA. Concerning forward-only estimation (FOE), it requires $N_s \times (2JM)^2 = 4N_s \times (JM)^2$ multiplications in calculating the correlation matrix $\hat{\mathbf{R}}_f$ shown in (19) and other computational demand is same as FBA. Thus the computation complexity of FOE is over twice of that of FFBE. From the simulation results in the next section, we verify these analyses.

V. SIMULATIONS AND DISCUSSIONS

In this section, simulations are presented to show the performance of the proposed FFBE. We compare the performance of the proposed FFBE with that of FBA and FOE for MIMO STBC-OFDM systems. In FOE and FBA, the correlation matrices are estimated by (19) and (15), respectively. While in FFBE, two sub-correlation matrices $(\mathbf{A}+j\mathbf{B})$ and $(\mathbf{A}-j\mathbf{B})$ are estimated by (32) and (33). In simulations, the signal-to-noise ratio (SNR) is defined by

$$SNR = \frac{E\left[\sum_{n=0}^{M-1}\left\|\mathbf{x}_i(n)-\boldsymbol{\eta}_i(n)\right\|^2\right]}{E\left[\sum_{n=0}^{M-1}\left\|\boldsymbol{\eta}_i(n)\right\|^2\right]} \tag{49}$$

The CIR is modeled as a wide-sense stationary uncorrelated scattering process composed of discrete paths in which the channel coefficients are assumed to be identically independent distributed complex Gaussian with zero mean and unit variance. For each Monte Carlo realization, we create random Rayleigh fading channels in which the channel coefficients are assumed to be statistically independent and have the same complex Gaussian distribution. The normalized mean square error (NMSE) (averaging on all channels) between the estimated and true channel responses is defined as

$$NMSE = \frac{\sum_{i=1}^{2}\sum_{l=0}^{L}\left\|\mathbf{h}_i(l)-\hat{\mathbf{h}}_i(l)\right\|^2}{\sum_{i=1}^{2}\sum_{l=0}^{L}\left\|\mathbf{h}_i(l)\right\|^2} \tag{50}$$

where $\mathbf{h}_i(l)$ and $\hat{\mathbf{h}}_i(l)$ represent the true and estimated CIR, respectively. In the following simulations, the performances of channel estimation in terms of NMSE and bit error rate (BER) are averaged over 100 Monte Carlo realizations. Moreover, we apply two ambiguity matrices for channel estimation, which are computed by "pilot SS" and "optimal SS" defined in (Yu et al., 2009).

Example 1

A two-user STBC-OFDM system composed of four transmitting antennas and three receiving antennas is considered here. The transmitted baseband signals are BPSK and IDFT block size is chosen to be 32. The number of pilot STBC symbols $N_P = 2$ and the maximum delay spread of all channels $L = 6$.

We first examine the SNR effect on the performance of FFBE. Figs. 2 and 3 show the NMSE and BER versus input SNR, respectively, for sample blocks $N_s = 200$. As we see, the proposed FFBE and FBA achieve a lower NMSE and BER than FOE method. This performance improvement of FFBE and FBA is consistent for SNR varied from 3 dB to 33 dB.

Next, we examine the convergence rate of the proposed FFBE. Figs. 4 and 5 present the NMSE and BER versus the number of block signals N_s, for input SNR = 15 dB. As we observe, FFBE and FBA achieve lower values of NMSE and BER with less number of block signals than FOE. For example, FFBE and FBA require 175 block signals to achieve 0.01 NMSE while FOE needs 350 block signals approximately, for ambiguity matrices in channel estimation calculated by utilizing "pilot SS". Similar results can be obtained from the plots in Fig. 5. We can find that the BER of FFBE and FBA with pilot SS is 0.0001 when number of block signals is equal to 200, while FOE with pilot SS requires approximately 400 block signals to achieve the same BER. The results imply the fast convergence rate of FFBE and FBA.

Example 2

In the experiment, we investigate the effect of DFT block size on the performance of FFBE. Concerning the dimension of correlation matrix, two receiving antennas, $J = 2$, are considered here and other simulation parameters are the same as those in Fig. 4. Figs. 6-9 display the NMSE versus the number

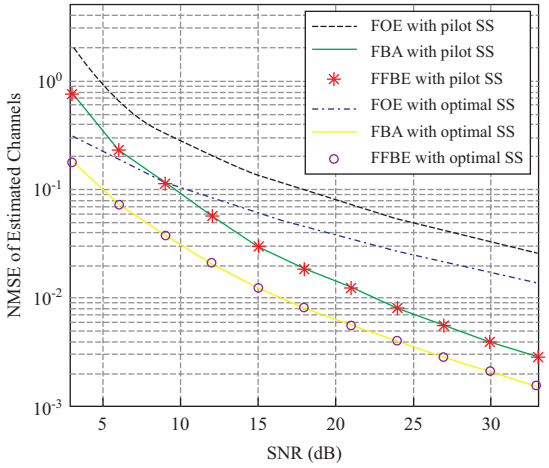

Fig. 2. Channel estimation performance versus SNR. ($J = 3$, $K = 2$, DFT size $N = 32$, and signal blocks $N_s = 200$).

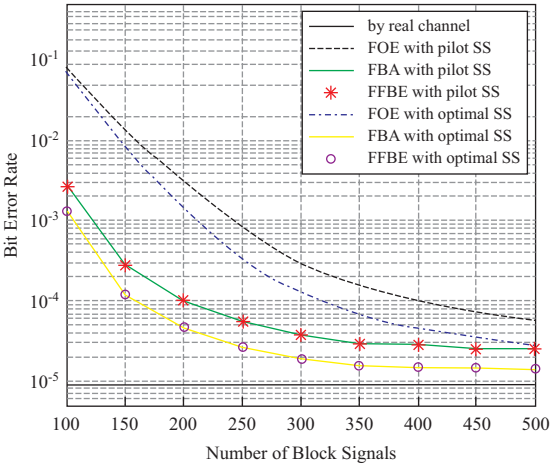

Fig. 5. BER versus number of block signals. (Simulation scenario same as Fig. 4.)

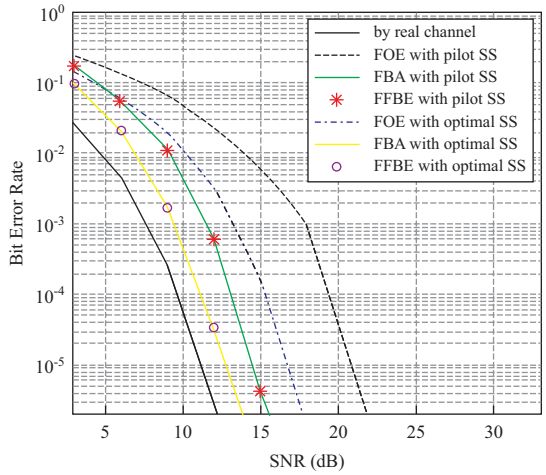

Fig. 3. BER versus SNR. (Simulation scenario same as Fig. 2).

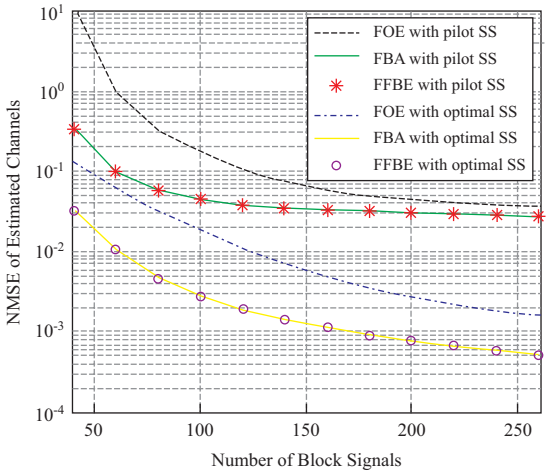

Fig. 6. Channel estimation performance versus number of block signals. ($J = 2$, $K = 2$, DFT size $N = 16$, $N_s = 200$ and SNR = 15 dB).

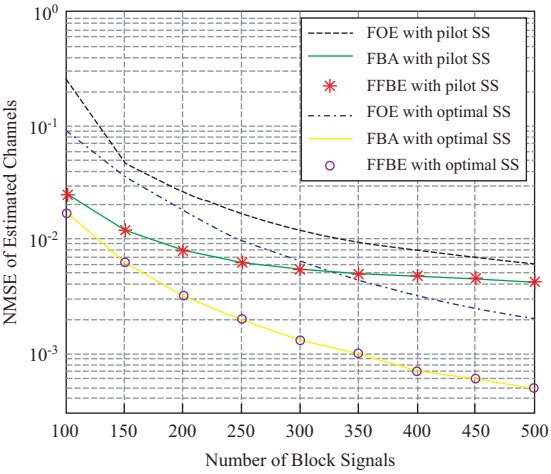

Fig. 4. Channel estimation performance versus number of block signals. (SNR = 15 dB, other simulation parameters same as Fig. 2).

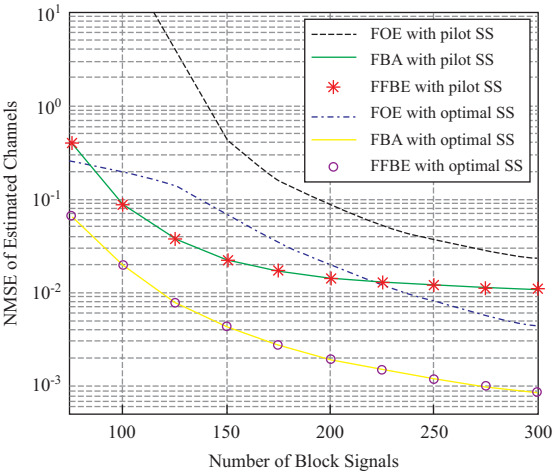

Fig. 7. Channel estimation performance versus number of block signals. (DFT size $N = 32$ and other simulation scenario same as Fig. 6).

Table 1. Comparison of execution time for the simulation.

No. of Block Signals	DFT Size	FFBE	FBA	FOE	Speed-up S_{p1}	Speed-up S_{p2}
$N_s = 300$	16	1.586	6.185	3.646	3.899	2.299
	32	6.008	21.414	15.963	3.564	2.657
	64	23.436	89.323	65.828	3.811	2.809
	128	102.517	481.886	314.438	4.701	3.067
$N_s = 600$	16	2.716	11.454	5.549	4.226	2.047
	32	8.752	33.872	21.267	3.87	2.43
	64	35.576	133.425	86.36	3.75	2.428
	128	147.495	727.407	482.609	4.931	3.272
Averaged Speedup					4.094	2.626

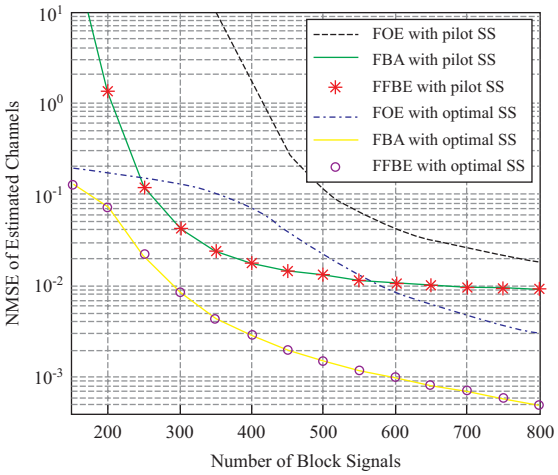

Fig. 8. Channel estimation performance versus number of block signals. (DFT size N=64 and other simulation scenario same as Fig. 6).

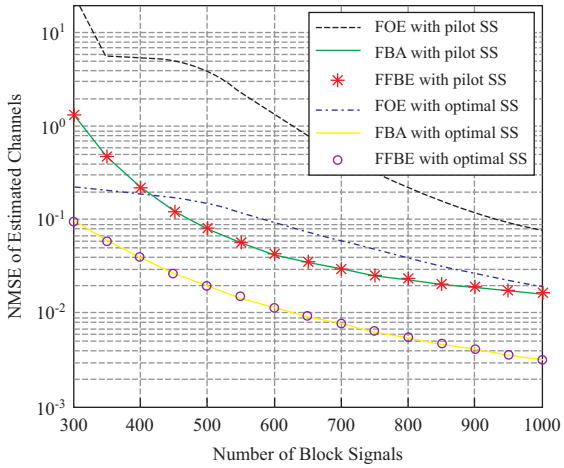

Fig. 9. Channel estimation performance versus number of block signals. (DFT size N=128 and other simulation scenario same as Fig. 6).

of block signal for DFT block size 16, 32, 64 and 128, respectively. From these figures, we observed that all three methods require larger block signals as the DFT block size increases. For instance, for FFBE and FBA with pilot SS, they require 90, 120, 300, and 550 block signals to achieve 0.05 NMSE corresponding to 16, 32, 64 and 128 DFT block size, respectively. Similarly, for FOE with pilot SS, the number of block signals are 180, 230, 600 and 1000 approximately, to achieve 0.05 NMSE for 16, 32, 64 and 128 DFT block size, respectively.

Next, the efficiency of the proposed FFBE is examined. We compare the execution time required for these three methods. Experiments have been conducted on the computer with CPU core i5-2450 (2.5G Hz). In simulations, the estimation methods were implemented by using MATLAB and elapsed time was measured by using functions "clock" and "etime" in MATLAB. The simulation scenarios are the same as those in Figs. 6-9. Execution time for different DFT block size is considered with 300 and 600 block signals. In order to evaluate the effectiveness of the proposed FFBE, we use the speedup index S_{pi} which is the ratio of execution time of FFBE to the other two methods, FBA and FOE,

$$S_{p1} = \frac{t_{fb}}{t_{ffb}} \text{ and } S_{p2} = \frac{t_f}{t_{ffb}} \tag{51}$$

where t_{ffb} denotes the averaged execution time of FFBE, t_{fb} and t_f represent the average execution time of FBA and FOE, respectively. The averaged execution time and speedup S_{pi} are shown in Table 1, in which execution time are averaged form 300 Monte Carlo realizations and averaged speedup are calculated from all simulation cases. Comparing the results in Table 1, we see that the averaged execution time of FFBE is almost one fourth and less than one half of that required in FBA and FOE, respectively. On average, FFBE achieves 4.1 and 2.6 times speedup of FBA and FOE, respectively. These results validate the efficiency of the proposed FFBE.

Example 3

The performance of FFBE for the multiuser STBC-OFDM systems is evaluated. The number of receiving antennas J is chosen as the user number K in following simulations. The number of block signals is 800, number of pilot symbols $N_p = K$ and other simulation parameters are the same as those in Example 1. The NMSE and BER versus the number of users are shown in Figs. 10 and 11. We can observe that the value of NMSE and BER increases as the user number grows. It is necessary to utilize more receiving data to estimate the subspace of correlation matrix as the user number increases which results in the increase of correlation matrix dimension. For a twenty-user system with the

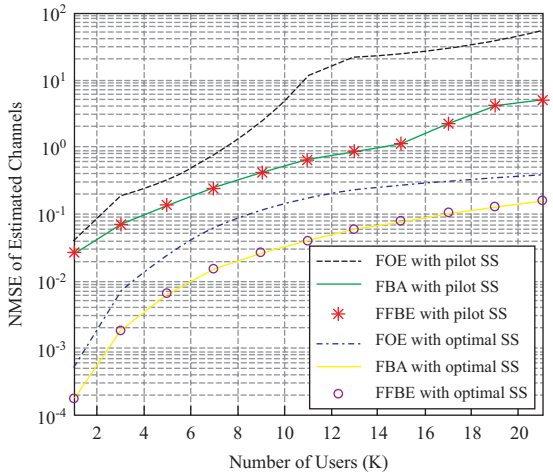

Fig. 10. Channel estimation performance versus number of users. ($J = K$, $N_s = 800$, $N_p = K$, DFT size $N = 32$, and SNR = 15 dB).

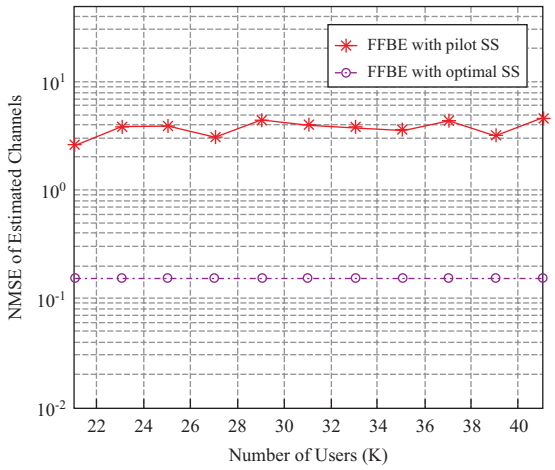

Fig. 12. Channel estimation performance versus number of users for FFBE. ($J = K$, $N_s = J^*M$, $N_p = K$, DFT size $N = 32$ and SNR = 15 dB).

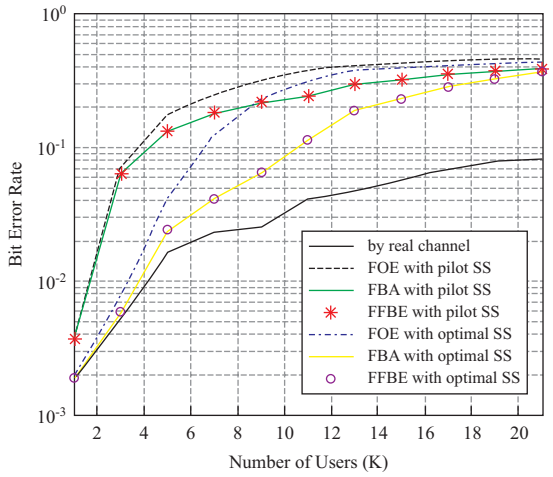

Fig. 11. BER versus number of users. (Simulation parameters same as Fig. 10).

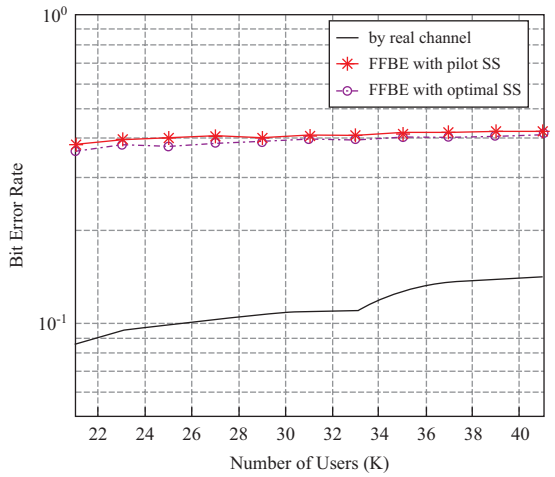

Fig. 13. BER versus number of users for FFBE. (Simulation scenario same as Fig. 12).

associated dimension of correlation matrix equal to 1520, 800 number of block signals is not enough to get a steady state value of estimated CIR.

In the simulations, we find that it is hard to keep increasing the user number because of the limited memory in MATLAB. Computing bottleneck occurs in performing singular value decomposition (SVD) of matrix $\mathbf{G}$ in (11). For DFT block size equal to 32, it is difficult to do CIR estimation by FBA and FOE if user number K is more than twenty. Without utilizing matrix $\mathbf{G}$, FFBE performs SVD of $\mathbf{E}_a$ and $\mathbf{E}_b$, of which dimension is half of matrix $\mathbf{G}$. Thus, FFBE can estimate CIR of systems with more users than FBA and FOE. We show the NMSE and BER versus the number of users for FFBE with user number $K > 20$ in Figs. 12 and 13. Concerning to achieve steady state estimation, the number of block signal is chosen to be $N_s = J^*M$ in the simulation. The results in Figs. 12 and 13 validate that the proposed FFBE still carries out CIR estimation for a MIMO system with J and K equal to 41.

VI. CONCLUSIONS

In the study, we explore the PI property of forward-backward correlation matrix and develop the FFBE technique for MIMO STBC-OFDM systems. We discover that all eigenvalues are pairing repeated and the corresponding eigenvectors possess symmetric characteristics of a matrix with PI property. From this observation, we develop a fast eign-decomposition method which calculates the associated eigen-components from two submatrices with half dimension of the original matrix. Then, the symmetric property of eigenvectors is employed to develop the FFBE estimation method of MIMO STBC-OFDM systems. Theoretic analysis and simulation results validate that the proposed FFBE method can achieve the same performance of FBA. But the computation complexity of the EFBE requires only one fourth

of FBA. Moreover, the proposed FFBE achieve a smaller NMSE of estimated CIR and lower BER than those by FOE. The computation complexity of the proposed FFBE is almost one half of that required in FOE. Simulations show that the proposed FFBE achieves over four times speedup of FBA on average and is favorable for strict memory constraint.

APPENDIX A

PROOF OF LEMMA 1

We give the proof of *Lemma* 1 in this appendix.

Proof

If $\mathbf{e}_i$ is the eigenvector of $\mathbf{S}_T$ with eigenvalue λ_i, substituting the symmetric structure of $\mathbf{S}_T = \begin{bmatrix} \mathbf{A} & \mathbf{B} \\ -\mathbf{B} & \mathbf{A} \end{bmatrix}$ into (25), and partitioning the eigenvector as $\mathbf{e}_i = \begin{bmatrix} \mathbf{e}_{i1} \\ \mathbf{e}_{i2} \end{bmatrix}$, we get

$$\begin{cases} \mathbf{A}\mathbf{e}_{i1} + \mathbf{B}\mathbf{e}_{i2} = \lambda_i \mathbf{e}_{i1} \\ \mathbf{A}\mathbf{e}_{i2} - \mathbf{B}\mathbf{e}_{i1} = \lambda_i \mathbf{e}_{i2} \end{cases} \tag{52}$$

Combine the above equations and obtain

$$\begin{aligned} (\mathbf{A} + j\mathbf{B})\mathbf{e}_{i1} + (\mathbf{B} - j\mathbf{A})\mathbf{e}_{i2} &= \lambda_i (\mathbf{e}_{i1} - j\mathbf{e}_{i2}) \\ &= (\mathbf{A} + j\mathbf{B})(\mathbf{e}_{i1} - j\mathbf{e}_{i2}) \end{aligned} \tag{53}$$

(53) indicates that λ_i is also the eigenvalue of matrix $(\mathbf{A} + j\mathbf{B})$ and the corresponding eigenvector $\mathbf{e}_{ai}$ is equal to $(\mathbf{e}_{i1} - j\mathbf{e}_{i2})$ for $\mathbf{e}_{i1} \neq j\mathbf{e}_{i2}$. Similarly, from (52), we get

$$\begin{aligned} (\mathbf{A} - j\mathbf{B})\mathbf{e}_{i1} + (\mathbf{B} + j\mathbf{A})\mathbf{e}_{i2} &= \lambda_i (\mathbf{e}_{i1} + j\mathbf{e}_{i2}) \\ &= (\mathbf{A} - j\mathbf{B})(\mathbf{e}_{i1} + j\mathbf{e}_{i2}) \end{aligned} \tag{54}$$

(54) means that the eigenvalue of matrix $(\mathbf{A} - j\mathbf{B})$ is equal to λ_i and the corresponding eigenvector $\mathbf{e}_{bi}$ is equal to $(\mathbf{e}_{i1} + j\mathbf{e}_{i2})$ for $\mathbf{e}_{i1} \neq -j\mathbf{e}_{i2}$. (53) and (54) show the relation of eigencomponents between the matrices $\mathbf{S}_T$ and $(\mathbf{A} \pm j\mathbf{B})$. The derivations could be performed in reverse direction.

If $\lambda_{a,i}$ and $\mathbf{e}_{ai}$ are the eigenvalue and eigenvector of matrix $(\mathbf{A} + j\mathbf{B})$, which satisfy

$$(\mathbf{A} + j\mathbf{B})\mathbf{e}_{ai} = \lambda_{a,i}\mathbf{e}_{ai},\ i = 1, \ldots, t \tag{55}$$

Premultiply (55) by j, and get

$$(\mathbf{A} + j\mathbf{B})\, j\mathbf{e}_{ai} = \lambda_{a,i} j\mathbf{e}_{ai},\ i = 1, \ldots, t \tag{56}$$

Combine (55) and (56), we have

$$\begin{bmatrix} \mathbf{A} & \mathbf{B} \\ -\mathbf{B} & \mathbf{A} \end{bmatrix} \begin{bmatrix} \mathbf{e}_{ai} \\ j\mathbf{e}_{ai} \end{bmatrix} = \lambda_{a,i} \begin{bmatrix} \mathbf{e}_{ai} \\ j\mathbf{e}_{ai} \end{bmatrix} = \mathbf{S}_T \begin{bmatrix} \mathbf{e}_{ai} \\ j\mathbf{e}_{ai} \end{bmatrix} = \lambda_{a,i} \begin{bmatrix} \mathbf{e}_{ai} \\ j\mathbf{e}_{ai} \end{bmatrix} \tag{57}$$

(57) indicates the eigencomponents of $\mathbf{S}_T$ can be obtained from the eigenvalue $\lambda_{a,i}$ and eigenvector $\mathbf{e}_{ai}$ of matrix $(\mathbf{A} + j\mathbf{B})$, that is

$$\begin{aligned} \lambda_i &= \lambda_{a,i} \\ \mathbf{e}_i &= \begin{bmatrix} \mathbf{e}_{ai} \\ j\mathbf{e}_{ai} \end{bmatrix}, \quad i = 1, \ldots, t \end{aligned} \tag{58}$$

Similarly, if $\lambda_{b,i}$ and $\mathbf{e}_{bi}$ represent the eigenvalue and eigenvector of matrix $(\mathbf{A} - j\mathbf{B})$, which satisfy

$$(\mathbf{A} - j\mathbf{B})\mathbf{e}_{bi} = \lambda_{b,i}\mathbf{e}_{bi},\ i = 1, \ldots, t \tag{59}$$

From (59) and multiplying (59) by -j, we get

$$\begin{bmatrix} \mathbf{A} & \mathbf{B} \\ -\mathbf{B} & \mathbf{A} \end{bmatrix} \begin{bmatrix} \mathbf{e}_{bi} \\ -j\mathbf{e}_{bi} \end{bmatrix} = \lambda_{b,i} \begin{bmatrix} \mathbf{e}_{bi} \\ -j\mathbf{e}_{bi} \end{bmatrix} = \mathbf{S}_T \begin{bmatrix} \mathbf{e}_{bi} \\ -j\mathbf{e}_{bi} \end{bmatrix} = \lambda_{b,i} \begin{bmatrix} \mathbf{e}_{bi} \\ -j\mathbf{e}_{bi} \end{bmatrix} \tag{60}$$

(60) shows the eigencomponents of $\mathbf{S}_T$ can be obtained for those of matrix $(\mathbf{A} - j\mathbf{B})$, that is

$$\lambda_i = \lambda_{b,i},\ \mathbf{e}_i = \begin{bmatrix} \mathbf{e}_{bi} \\ -j\mathbf{e}_{bi} \end{bmatrix},\ i = 1, \ldots, t \tag{61}$$

We then prove eigenvector $\mathbf{e}_i$ obtained from $\mathbf{e}_{ai}$, $i = 1, \ldots, t$, eigenvector of $(\mathbf{A} + j\mathbf{B})$, are distinct from $\mathbf{e}_{bi}$, $i = 1, \ldots, t$, eigenvector of $(\mathbf{A} - j\mathbf{B})$. Assume that eigenvector $\mathbf{e}_i$ obtained from $(\mathbf{A} + j\mathbf{B})$ has the same direction as one eigenvector of $(\mathbf{A} - j\mathbf{B})$, which satisfy

$$\begin{bmatrix} \mathbf{e}_{ai} \\ j\mathbf{e}_{ai} \end{bmatrix} = k \begin{bmatrix} \mathbf{e}_{bi} \\ -j\mathbf{e}_{bi} \end{bmatrix} \tag{62}$$

Rewrite (62) as

$$\begin{cases} \mathbf{e}_{ai} = k\mathbf{e}_{bi} \\ \mathbf{e}_{ai} = -k\mathbf{e}_{bi} \end{cases} \tag{63}$$

(63) implies $k = 0$. Thus, we validate that half of eigenvectors $\mathbf{e}_i$, $i = 1, \ldots, 2t$ of $\mathbf{S}_T$ can be obtained from $\mathbf{e}_{ai}$, and half of $\mathbf{e}_i$ obtained from $\mathbf{e}_{bi}$.

(58) and (61) give the proof of *Lemma* 1.

REFERENCES

Agrawal, D., V. Tarokh, A. Naguib and N. Seshadri (1998). Space-time coded OFDM for high data- rate wireless communication over wideband channels. Proc. IEEE Veh. Technol. Conf., VTC 98, Ottawa, Ont., 2232-2236.

Akansu, A. N., P. Duhamel, X. Lin and M. Courville (1998). Orthogonal transmultiplexers in communication: a review. IEEE Trans. on Sig. Proc. 46(4), 979-995.

Alamouti, S. M. (1998). A simple transmit diversity technique for wireless communications. IEEE J. Sel. Areas Commun 16 (8), 1451-1458.

Ali, H., A. Doucet and Y. Hua (2004). Blind SOS subspace channel estimation and equalization techniques exploiting spatial diversity in OFDM systems. Digit. Signal Process 14(2), 171-202.

Bolcskei, H. (2006). MIMO-OFDM wireless systems: basics, perspectives, and challenges. IEEE Wireless Commun 13(4), 31-37.

Dash, D., A. Agarwal and K. Agarwal (2013). Performance analysis of OFDM based DVB-T over diverse wireless communication channels. International J. of Elec. and Commun. Eng. 6(1), 131-141.

Doufexi, A., S. Armour, M. Butler, A. Nix, D. Bull, J. McGeehan and P. Karlsson (2002). A comparison of the HIPERLAN/2 and IEEE 802.11a wireless LAN standards. IEEE Commun. Mag 40(5), 172-180.

Gesbert, D., M. Shafi, D. Shiu, P. J. Smith and A. Naguib (2003). From theory to practice: an overview of MIMO space-time coded wireless systems. IEEE J. Sel. Areas Commun 21(3), 281 - 302.

Gong, Y. and K. B. Letaief (2003). Low complexity channel estimation for space-time coded wideband OFDM systems. IEEE Trans. Wireless Commun 2(5), 876-882.

Hong, Y., E. Viterbo and J. C. Belfiore (2007). Golden space-time trellis coded modulation. IEEE Trans. Inf. Theory 53(5), 1689-1705.

IEEE Std. 802.11 (2016). 802.11-2016-IEEE standard for information technology-telecommunications and information exchange between systems local and metropolitan area networks-specific requirements - Part 11: wireless LAN Medium Access Control (MAC) and Physical Layer (PHY) specifications. IEEE, doi: 10.1109/IEEESTD.2016.7786995.

Lu, B. and X. Wang (2000). Space-time code design in OFDM systems. Proc. IEEE Global Telecommunications Conf., San Francisco, CA., 1000-1004.

Lu, B., X. Wang and Y. Li (2002). Iterative receivers for space-time block-coded OFDM systems in dispersive fading channels. IEEE Trans. Wireless Commun 1(2), 213–225.

Lu, L. G. Y. Li, A. L. Swindlehurst, A. Ashikhmin and R. Zhang (2014). An overview of massive MIMO: benefits and challenges. IEEE J. Sel. Topics in Signal Processing 8(5), 742 - 758.

Ming, J. and L. Hanzo (2007). Multiuser MIMO-OFDM for next-generation wireless systems. Proc. IEEE 95(7), 1430–1469.

Muquet, B., Z. Wang, G. B. Giannakis, M. de Courville and P. Duhamel (2001). Cyclic prefixing or zero padding for wireless multicarrier transmissions?. IEEE Trans. Commun 50(12), 2136-2148.

Naguib, A. F., N. Seshadri and A. R. Calderbank (2000). Increasing data rate over wireless channels. IEEE Signal Process. Mag. 17(3), 76-92.

Nee, R. V. and R. Prasad (2000). OFDM for Wireless Multimedia Communications. London, U.K.: Artech House.

Paulraj, A. J., D. A. Gore, R. U. Nabar and H. Bolcskei (2004). An overview of MIMO Communications - A key to gigabit wireless. Proceedings of the IEEE 92(2), 198-218.

Sklavos, A., T. Weber, E. Costa, H. Haas and E. Schulz (2002). Joint detection in multi-antenna and multi-user OFDM systems. In: Multi-Carrier Spread-Spectrum and Related Topics, edited by Fazel, K. and Kaiser, S., Boston, MA: Kluwer.

Swindlehurst, A. L., E. Ayanoglu, P. Heydari and F. Capolino (2014). Millimeter-wave massive MIMO: the next wireless revolution?. IEEE Commun. Mag. 52(9), 56-62.

Tarokh, V., N. Seshadri and A. R. Calderbank (1998). Space-time codes for high data rate wireless communications: performance criterion and code construction. IEEE Trans. Inf. Theory 44(2), 744-765.

Tarokh, V., N. Seshadri and A. R. Calderbank (1999). Space-time block codes from orthogonal designs. IEEE Trans. Inf. Theory 45(5), 1456-1467.

Wang, H., X. Xia, Q. Yin and B. Li (2009). A family of space-time block codes achieving full diversity with linear receivers. IEEE Trans. Commun 57(12), 3607-3617.

Yu, J. L. and Y. C. Lin (2009). Space-time-coded MIMO ZP-OFDM systems: semiblind channel estimation and equalization. IEEE Trans. Circuits Syst. I, Reg. Papers 56(7), 1360-1372.

Zeng, Y. H. and T. S. Ng (2004). A semi-blind channel estimation method for multi-user multi-antenna OFDM systems. IEEE Trans. Signal Process 52(5), 1419-1429.

Zeng, Y. H., W. H. Lam and T. S. Ng (2006). Semi-blind channel estimation and equalization for MIMO space-time coded OFDM. IEEE Trans. Circuits Syst. I, Reg. Papers 53(2), 463-374.

Zhou, S., B. Muquet and G. B. Giannakis (2002). Subspace-based (semi-)blind channel estimation for block precoded space-time OFDM. IEEE Trans. Signal Process 50(5), 1215-1228.